J Wood Sci (2012) 58:408–416
DOI 10.1007/s10086-012-1275-5

ORIGINAL ARTICLE

Dynamic responsive characteristics of nailed plywood–timber joints under harmonic vibrations

Takuro Hirai · Takeyoshi Uematsu · Yoshihisa Sasaki · Masahiko Toda · Okumu Gordon Wanyama · Kei Sawata

Received: 13 February 2012 / Accepted: 25 May 2012 / Published online: 17 June 2012

Abstract Dynamic tests of nailed plywood–timber joints are conducted under harmonic vibrations from 2 to 7 Hz. The principal results are as follows: under dynamic loading, nailed plywood–timber joints may break in low-cyclic bending fatigue failure of nails besides the other failure modes typical under static loading. The dynamic response of nailed plywood–timber joints is clearly dependent upon both the input frequency and the acceleration. These responsive characteristics arise from the nonlinear load–slip relationships and the characteristic cyclic stiffness degradation of nailed joints; that is, the cyclic degradation of the equivalent linear stiffness decreases the resonant frequencies of the same joints, which results in a transition of dynamic responses. It indicates that frequency components of seismic waves resonant to the frequencies corresponding to safety-limit stiffness of nailed joints may lead them to critical failures, even if the accelerations do not exceed the accelerations equivalent to the static damage-limit resistance.

Keywords Nailed plywood–timber joints · Harmonic vibration · Dynamic response · Nonlinear load–slip relationship · Frequency dependence

T. Hirai (✉) · Y. Sasaki · O. G. Wanyama · K. Sawata
Laboratory of Timber Engineering, Research Faculty of Agriculture, Hokkaido University, Sapporo 060-8589, Japan
e-mail: hirai@for.agr.hokudai.ac.jp

T. Uematsu
Northern Regional Building Research Institute, Hokkaido Research Organization, Asahikawa 078-8801, Japan

M. Toda
Forest Products Research Institute, Hokkaido Research Organization, Asahikawa 071-0198, Japan

Introduction

Nailed joints are widely used as a principal choice for structural joints in timber constructions. The static lateral resistance of nailed joints of various kinds, therefore, has been investigated from both the academic and the practical viewpoints [1–6]. The dynamic behavior of nailed joints, on the other hand, has not been clarified enough to be applied to the seismic design of timber constructions.

The dynamic resistance of timber joints has been discussed primarily by converting dynamic forces into equivalent static forces as products of given mass and input accelerations [7]. This simple conversion is convenient for practical design, however, the actual dynamic behavior is more complicated. A principal incompatibility between actual dynamic resistance and equivalent static resistance is frequency dependence in dynamic response. The current design codes in Japan provide design procedures that take into consideration this frequency dependence related to the load-deformation characteristics of entire structures or principal structural elements [8]. Another important behavior of timber joints under dynamic forces is the low-cyclic bending fatigue failure of metal fasteners. The low-cyclic bending fatigue failure, which also is frequency dependent, has occasionally been observed in shaking table tests of full-scale wooden structures and structural elements, however, this observation has not been discussed in detail until now.

Because timber constructions are multiple-joint systems consisting of various joints that have different responsive characteristics, the dynamic response of entire structures under seismic forces is the result of the successive transition of the dynamic response of each joint and the resultant successive force redistribution among the joints.

From this background, shaking table tests of nailed plywood–timber joints were conducted under harmonic

waves of various frequencies using a uniaxial shaking table.

Experiment

Materials

The nailed plywood–timber joints were assembled using 9.5-mm thick Karamatsu (*Larix kaempferi*) plywood, Todomatsu (*Abies sachalinensis*) timber, and CN50 common nails (2.87 mm in nominal diameter and 51.0 mm in nominal length). The density and the moisture content of the Karamatsu plywood ranged from 0.47 to 0.54 g/cm^3 (0.51 g/cm^3 on average) and from 6.9 to 8.3 % (7.5 % on average), and those of the Todomatsu timber ranged from 0.36 to 0.45 g/cm^3 (0.40 g/cm^3 on average) and from 7.3 to 8.9 % (8.2 % on average), respectively. These test materials were divided evenly among all test conditions including preliminary static tests based on the densities of the materials.

Preliminary static single-shear test

Twelve nailed plywood–timber joints were tested in static single shear as shown in Fig. 1 in advance of the dynamic tests. In a static test, a plywood side member of 45 mm in width and 255 mm in length was fastened with a CN50 nail onto a timber main member of 60 mm in depth, 40 mm in width and 300 mm in length according to the standard end and side distances [9]; that is, the end distance was 6 times the nominal nail diameter of 2.87 mm in the plywood side members and 15 times in the timber main members, and the side distance was about 7 times the nail diameter in both members. The nails were hammered moderately so as to avoid initial friction between the members [9]. The assembled specimens were loaded monotonically parallel to both the grain of the timber main members and the grain of the surface veneers of the plywood side members using a hydraulic testing system until failure occurred in the general way of static single-shear tests [2, 4]. The static load–slip curves of the 12 specimens were averaged into the control load–slip curve. The control static maximum load, two-thirds and one-third of it, and the equivalent linear secant stiffness at these three load levels were roundly determined from this control curve.

Dynamic single-shear tests

Dynamic single-shear tests were conducted under harmonic waves using a uniaxial hydraulic shaking table as shown in Fig. 2. The full capacity, the maximum displacement and the maximum velocity of the shaking table were ±9.6 kN,

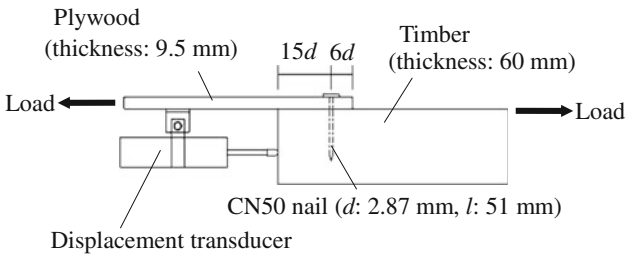

Fig. 1 Static single-shear test

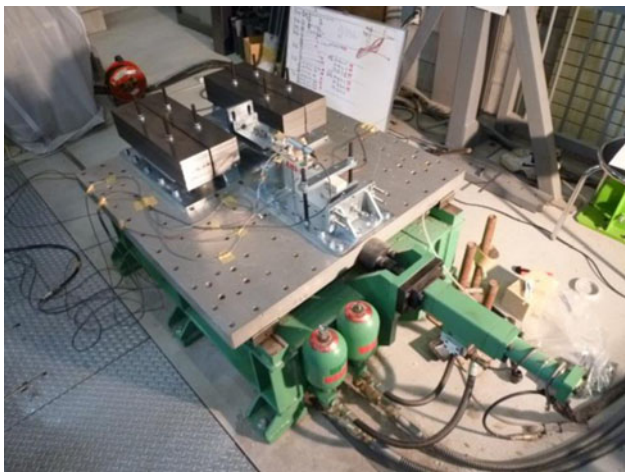

Fig. 2 Shaking table and test setup used in dynamic single-shear test

±50 mm, and 590 mm/s, respectively. The specimens were assembled in the same way as the preliminary static tests except for the depth and the length of the timber main members, which were altered to 125 and 240 mm, respectively, to fit the steel base (A) fixed onto the shaking table as shown in Fig. 3. The timber main member was supported tightly on this steel base. The plywood side member was fixed to the steel base (B) on the opposite side, which was placed on a pair of sliding rails with two pairs of bearings as shown in Fig. 3 to allow the smooth motion of mass, free from the motion of the shaking table. The mass was adjusted using removable steel plates fixed to the steel base (B).

The input acceleration at the timber main member fixed to the shaking table and the responsive acceleration at the plywood side member fixed to the sliding mass were measured using strain gauge accelerometers with a capacity of 2 G. The relative slip between the side member and the main member was measured synchronously with the accelerations using a displacement transducer with a 50-mm stroke. The acceleration on the shaking table was also measured to verify that the timber main member was firmly fixed onto the shaking table.

The given mass (m), input accelerations (a), and frequencies of the harmonic waves were determined by paying comprehensive consideration to the static maximum

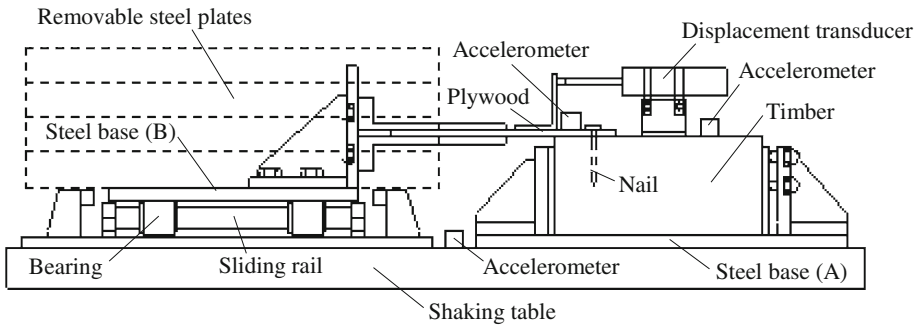

Fig. 3 Details of dynamic single-shear test

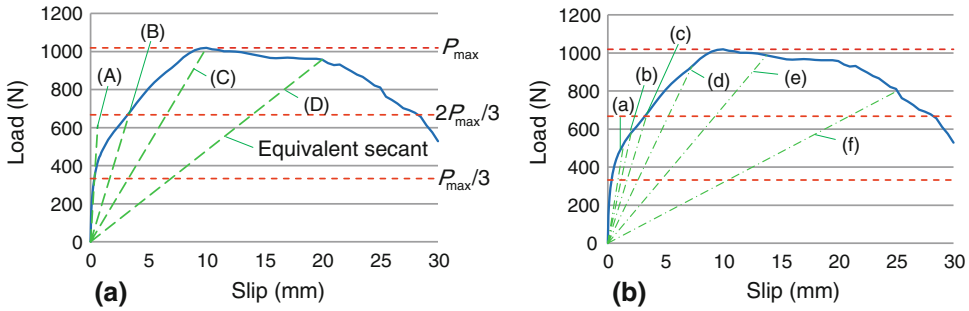

Fig. 4 Control static load–slip curve and equivalent linear secant stiffness. **a** Equivalent linear secant stiffness at one-third, two-thirds and three-thirds of the static maximum load and joint slip of 20 mm corresponding to frequencies of (*A*) 11.2 Hz, (*B*) 5.0 Hz, (*C*) 3.6 Hz and (*D*) 2.5 Hz. **b** Equivalent linear secant stiffness corresponding to frequencies of (*a*) 7 Hz, (*b*) 6 Hz, (*c*) 5 Hz, (*d*) 4 Hz, (*e*) 3 Hz and (*f*) 2 Hz

load and the successive transition of the equivalent linear secant stiffness (k) along the control static load–slip curve, shown later (see Fig. 4), and the capacity of the shaking table used in this study. This is because the variables above are naturally dependent on each other as shown in the following equations.

$$F = ma \tag{1}$$

$$k = \frac{F}{s} \tag{2}$$

$$f_r = \frac{1}{2\pi}\sqrt{\frac{k}{m}} \tag{3}$$

where F = equivalent static load (see Fig. 4), m = given mass, a = input acceleration, k = equivalent linear secant stiffness (see Fig. 4), s = joint slip (see Fig. 4), and f_r = resonant frequency (see Fig. 4).

As a result, the given mass and the input accelerations were determined to be 202 kg and 165 gal (cm/s^2) (0.17 G), 330 gal (cm/s^2) (0.34 G) and 495 gal (cm/s^2) (0.51 G). The products of the given mass by the input accelerations above were equivalent to one-third, two-thirds and three-thirds of the control static maximum load, respectively. The frequencies of the harmonic waves were determined to be 2, 3, 4, 5, 6 and 7 Hz (see Fig. 4b). These frequencies were within the general distribution of base shear spectra [10].

For each testing condition, 6 specimens were tested one-dimensionally in the direction parallel to both the grains of the timber main members and the surface veneers of the plywood side members. The specimens were shaken continuously to failure or for 150 s if clear failures were not found.

Results and discussion

Preliminary static single-shear tests

Figure 4a shows the control static load–slip curve averaged from the load–slip curves of 12 specimens. From this control load–slip curve, one-third, two-thirds and three-thirds of the control static maximum load were roundly estimated to be 333, 667 and 1000 N, respectively. The equivalent linear stiffness calculated from the secants at one-third, two-thirds and three-thirds of the control static maximum load and the load at the joint slip of 20 mm were 1000, 202, 101 and 48 N/mm (see the secants shown in Fig. 4a). The equivalent linear stiffness above

corresponded to the resonant frequency of 11.2, 5.0, 3.6 and 2.5 Hz, respectively [see Eq. (3)]. The control load–slip curve is shown again with the equivalent secants corresponding to the resonant frequencies of 7, 6, 5, 4, 3 and 2 Hz in Fig. 4b.

The standard short-term allowable lateral resistance according to the current Japanese design standard for timber structures [9] of nailed plywood–timber joints with Todomatsu timber and Karamatsu plywood is 66 % of 667 N, which is two-thirds of the control static maximum load. In this design standard, the allowable lateral resistance is conservatively given for the lower limit specific gravities of the materials. Because the specific gravities of the materials used in this study were higher than the lower limit values, the short-term allowable lateral resistance was adjusted to the actual specific gravities. The resultant short-term allowable resistance was 494 N, 74 % of 667 N [9]. As a result, one-third, two-thirds and three-thirds of the control maximum load corresponded to 0.68, 1.36 and 2.03 times the short-term allowable lateral resistance adjusted to the actual specific gravities of the materials. In this study, the rounded average maximum load was adopted as the control value with no conservative estimation. This was due to the consideration that an underestimation of the input forces would result in an overestimation of the dynamic resistance.

Dynamic single-shear tests

Figure 5 shows examples of the time series of the actual input accelerations at the timber main members and the responsive accelerations at the plywood side members for the initial 10 s. The designed input acceleration for these specimens was 330 gal, which was equivalent to two-thirds of the control static maximum load. The nailed plywood–timber joints had the characteristic frequency dependence as shown in the figure. Under a 2 Hz harmonic wave, the specimens responded in resonance with this frequency and failed within 20 cycles without reaching steady-state vibration. The specimens failed in a typical static failure mode, nail-head-pull-through occasionally accompanied by shear failure of the plywood side members. Under waves with frequencies from 3 to 7 Hz, on the other hand, the specimens failed in low-cyclic bending fatigue of nails [11]. Particularly under a wave of 3 Hz, the nails broke within 60 cycles in all specimens. The specimen vibrated under a wave of 3 Hz (Fig. 5b) failed at about 6 s (less than 20 cycles) and the intense amplitude after 8 s in the figure was the result of the free motion of the sliding mass already detached from the main member. The bending fatigue failure of the nails took place at cross sections about 10 mm from the edges of the timber main members, and the actual diameter of 2.85 mm was narrowed to 2.73 mm

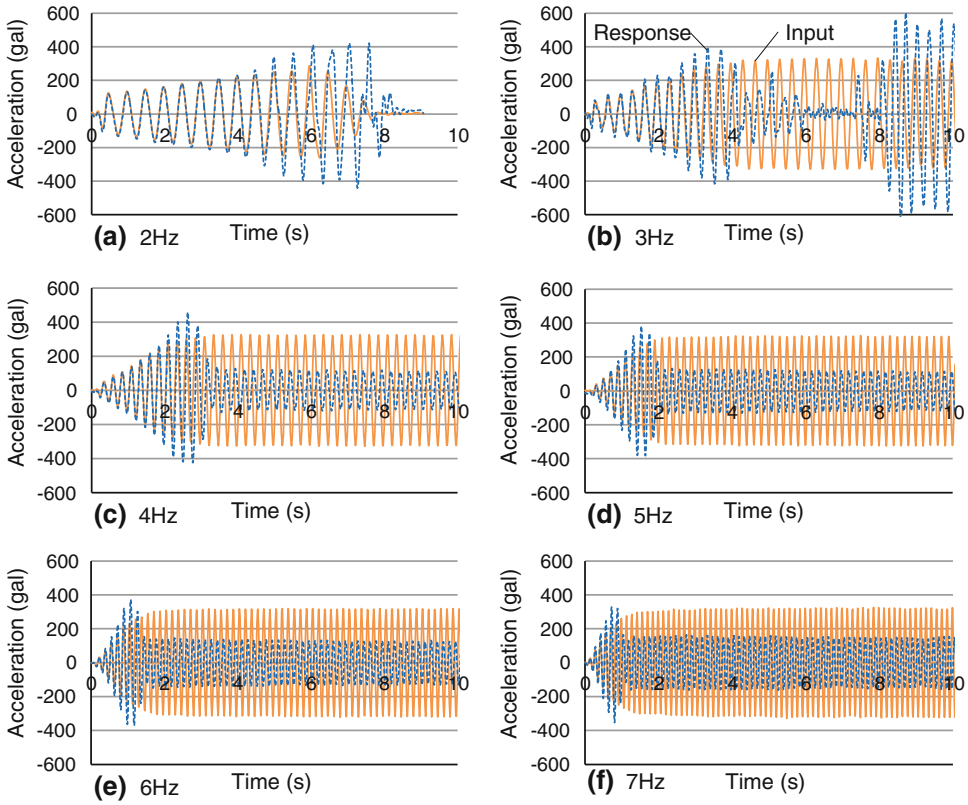

Fig. 5 Examples of time series of input accelerations of timber main members (330 gal) and responsive accelerations at plywood side members

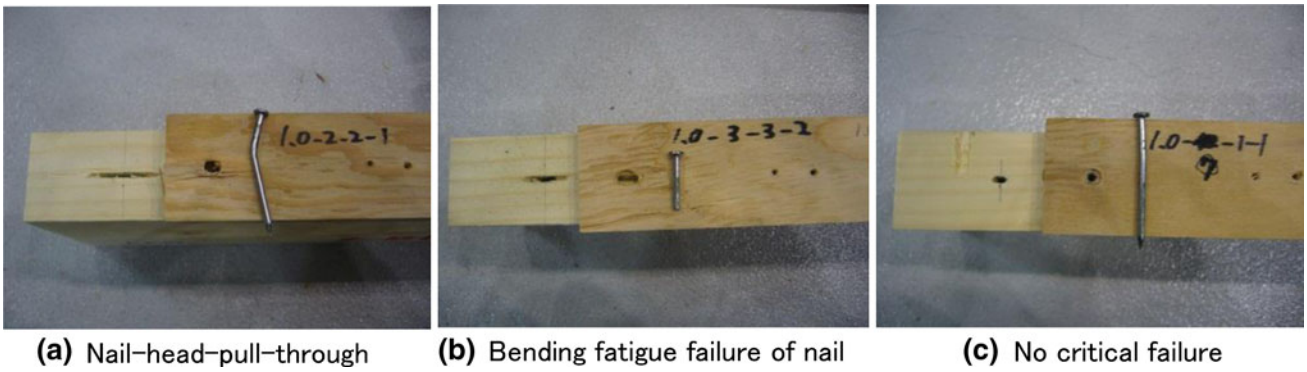

Fig. 6 Typical failure modes

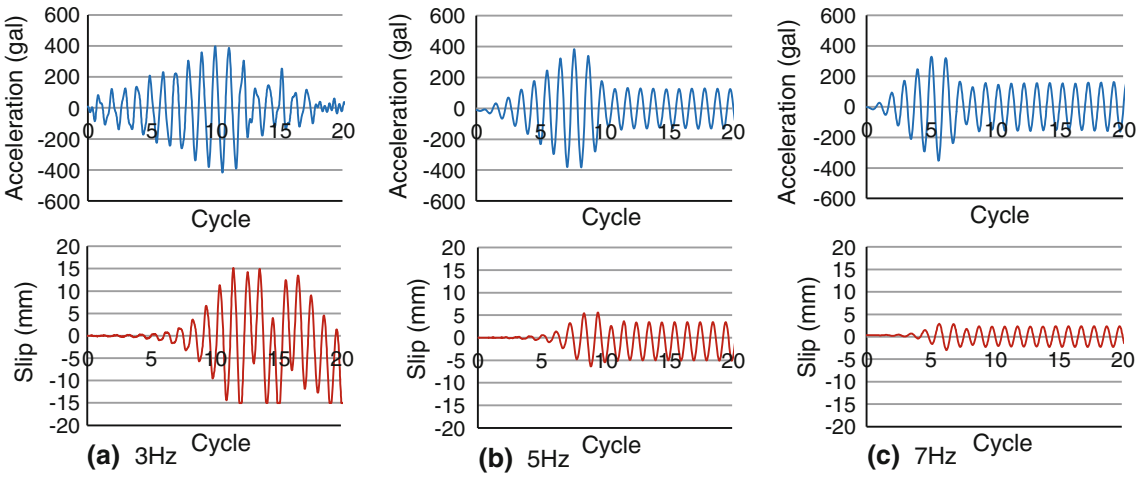

Fig. 7 Responsive accelerations at side members and slips between main members and side members for input accelerations of 330 gal under harmonic waves of 3, 5 and 7 Hz

at the broken cross sections on average. Under frequencies from 3 to 7 Hz, the specimens responded sensitively once, and then responded dully and vibrated steadily until failure as shown in Fig. 5. Bending fatigue failure of the nails took more cycles as the frequency increased from 3 to 7 Hz. Under a wave of 7 Hz, five-sixths of the specimens survived the shaking for 150 s with no critical failure for this input acceleration corresponding to two-thirds of the control static maximum load. Figure 6 shows typical failures: nail-head-pull-through, and low-cyclic bending fatigue failure of a nail. A typical example of a specimen after shaking for 150 s under a wave of 7 Hz is also shown in the figure.

The results above are related to the responsive joint slips shown in Fig. 7 for 3, 5 and 7 Hz. These joint slips are simultaneous with the responsive accelerations shown again in Fig. 7 for the same input accelerations shown in Fig. 5. In Fig. 7, the accelerations and the slips are plotted in cycles instead of time (s). Figure 7 shows clearly the frequency dependence of the responsive joint slips.

The characteristic dynamic responses of the joints depended upon the input frequency are made clearer by observing the responsive acceleration–slip curves shown in Fig. 8. In this figure, the control static load–slip curves (see Fig. 4) are shown again by converting static loads into equivalent accelerations together with the equivalent slips and secants resonant to each input frequency from 2 to 7 Hz. Figure 8 shows that the dynamic cyclic loops shift gradually to nearly inside the static envelope curves. In this figure, a characteristic difference can be seen in the dynamic response between the frequencies of 2 and 3 Hz. For the frequency of 2 Hz, both the responsive acceleration and slip increased with every cycle accompanied by a cyclic degradation of the equivalent linear stiffness. This behavior was gradual in the early phase of the cyclic response, and became more intense as the resultant equivalent linear stiffness came closer to the equivalent secant stiffness in Fig. 8a. For this frequency, the plywood side members failed in nail-head-pull-through occasionally accompanied by plywood shear started from the edges of

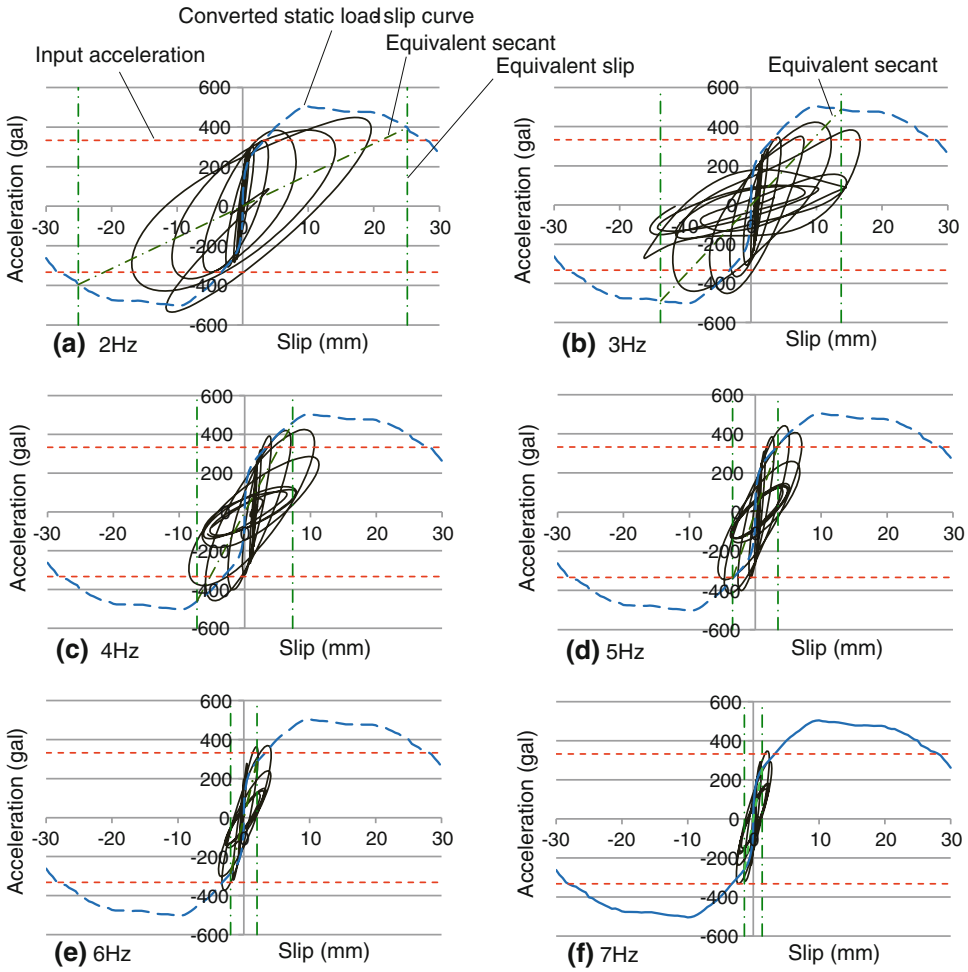

Fig. 8 Examples of dynamic responsive acceleration–slip loops for input accelerations of 330 gal equivalent to two-thirds of static maximum load

nail holes preceding the bending fatigue failures of the nails (see Fig. 6a). A similar responsive behavior was observed also for the frequency of 3 Hz until the degraded equivalent linear stiffness reached the equivalent secant stiffness in Fig. 8b. Past this early phase, however, the responsive acceleration decreased every cycle and the dynamic cyclic loop shifted apart from the static envelope curve. The resultant equivalent stiffness of the cyclic loops, which was lower than the equivalent secant stiffness in Fig. 8b, dulled the dynamic response of the nailed joints. This responsive behavior saved the joints from typical static failures and the joints finally failed in low-cyclic bending fatigue of the nails at the cross sections of the plastic hinges after a number of cycles (see Fig. 6b). These characteristic responses indicate that the dynamic cyclic loops shift along the static envelope curves, which are amplified at every cycle, when the nailed joints finally fail in the typical static failure modes (see Fig. 8a). This dynamic behavior results in comparatively larger responsive slips. If the cyclic loops shift downward apart from the static envelope curves (see Fig. 8b), on the other hand, the nailed joints hardly fail in the typical static failure modes. In these cases, however, the nailed joints may fail in the low-cyclic bending fatigue of the nails after a number of cycles. The characteristic responsive behavior for frequencies of more than 3 Hz was qualitatively similar to that for 3 Hz (see Fig. 8c–f), although the responsive slips decreased as the frequency increased.

These characteristic responses arise from the nonlinear load–slip relationships and the cyclic stiffness degradation of the nailed joints [2, 3]. That is, the cyclic decrease of the responsive accelerations and/or the cyclic increase of the responsive slips cause the gradual decline of the equivalent linear stiffness. This transition of the equivalent linear stiffness gradually decreases the resonant frequencies of the joints as indicated in Figs. 4 and 8. During the early phase of the dynamic response, the joints respond once sensitively to higher frequencies when the transitional resonant frequencies of the joints synchronize with those frequencies. After this early phase, however, the cyclic degradation of the equivalent stiffness decreases the resonant frequencies of the joints, which results in a dull

response to the higher frequencies. The cyclic degradation of the equivalent stiffness, on the other hand, brings gradually the resonant frequencies of the joints close to the lower frequencies, which causes their critical failures.

The results above are for an input acceleration of 330 gal, which is equivalent to two-thirds of the control static maximum load. To compare the responsive characteristics on a common basis among all input accelerations and frequencies, the measured maximum responsive accelerations were converted into their ratios to the measured maximum input accelerations. The resultant average maximum responsive acceleration ratios depended clearly on both the input accelerations and the frequencies or combinations of them [12] as shown in Fig. 9. When the input acceleration was 165 gal, the joints responded sensitively to frequencies from 3 to 7 Hz and the responsive acceleration ratios tended to increase slightly as the frequency increased. This input acceleration was equivalent to one-third of the control static maximum load, at which the upper limit of the responsive acceleration was about 3.0 and the equivalent resonant frequency was 11.2 Hz (see Fig. 4). When the input acceleration was 330 gal, the joints responded most sensitively to a frequency of 2 Hz and responded gradually more dully as the frequency increased. This input acceleration was equivalent to two-thirds of the control static maximum load, at which the upper limit of the responsive acceleration ratio was about 1.5 and the equivalent resonant frequency was 5.0 Hz.

The upper limit of the responsive acceleration ratio is naturally about 1.0 when the input acceleration is 495 gal, which is equivalent to the control static maximum load and the equivalent resonant frequency is 3.6 Hz. The responsive acceleration ratio for this input acceleration, defined as the ratio of the measured maximum responsive acceleration to the measured maximum input acceleration, however, is greater than 1.0 for a frequency of 2 Hz as shown in Fig. 9. In shaking table tests, it takes a number of cycles to reach steady accelerations as shown in Figs. 5 and 7. Under a frequency of 2 Hz, the joints failed at average actual input accelerations of 305 and 321 gal before they reached the assumed steady values of 330 and 495 gal, respectively. A responsive acceleration ratio greater than 1.0 for the steady input acceleration of 495 gal is the result of this failure behavior. The measured maximum responsive acceleration for this input acceleration was 485 gal on average, which did not exceed the assumed upper limit value of 495 gal. Under frequencies from 3 to 7 Hz, the input acceleration reached the steady value before the joints failed. For an input acceleration of 495 gal, as a result, the responsive acceleration ratios dropped to less than 1.0, and they decreased gradually as the frequency increased from 3 to 7 Hz. For this input acceleration, the joints initially responded sensitively below the steady acceleration state, and then the resultant cyclic stiffness degradation dulled their response and lasted them for a number of cycles under the steady acceleration for these frequencies. This responsive behavior resulted in responsive acceleration ratios of not exceeding 1.0.

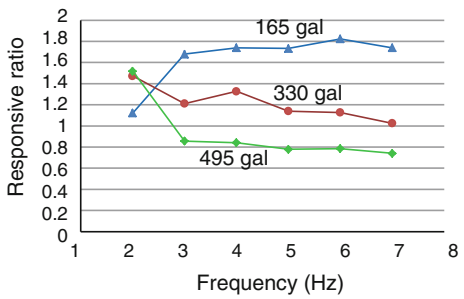

Fig. 9 Responsive acceleration ratios

The frequency dependence of the responsive accelerations and slips resulted in the cycles at the ultimate failures of the specimens and their failure modes as shown in Table 1. The boldface and italic entries in Table 1 show, respectively, low-cyclic bending fatigue failure and nail-head-pull-through with occasional plywood shear. The cycles with "a" symbols show that no critical failures were observed after shaking for 150 s. The average cycles of the 6 specimens shown in Table 1 are shown again in Fig. 10, where the outline markers and the broken lines show that at least some of the specimens did not critically fail after shaking for 150 s. Table 1 and Fig. 10 show the relative sensitivities of the dynamic responses and the obvious frequency dependence of the nailed plywood–timber joints among the combinations of input acceleration and frequency. The input acceleration equivalent to the standard short-term allowable lateral resistance [9] adjusted to the specific gravities of the test materials is about 244 gal, which lies between 167 gal and 330 gal.

An important result in Table 1 and Fig. 10 is that the dynamic response of the nailed plywood–timber joints is relatively more sensitive to input frequency than input acceleration. Another important result is that the most severe frequency that causes the bending fatigue failure of nails does not coincide with the most severe frequency that causes a typical failure in static loading, nail-head-pull-through.

The general view of the test results indicates that nailed joints are likely damaged by the frequency components of seismic waves close to their higher resonant frequencies below the damage-limit or serviceability-limit resistance. However, the nailed joints are ultimately broken by the lower frequency components of seismic waves, to which damaged joints with degraded stiffness resonate. The transition of the responsive behavior of the nailed joints

Table 1 Cycles at failure of each specimen

Input acceleration (equivalent static load)	Frequency (Hz)					
	2	3	4	5	6	7
165 gal (one-third of static maximum resistance)	300[a]	**118**	**343**	750[a]	900[a]	1050[a]
	35	**157**	**167**	**344**	900[a]	1050[a]
	300[a]	**130**	**128**	**387**	900[a]	1050[a]
	300[a]	**52**	**157**	**720**	900[a]	1050[a]
	56	**141**	**284**	750[a]	900[a]	1050[a]
	300[a]	**199**	**368**	750[a]	900[a]	1050[a]
Average	215[b]	133	241	617[b]	900[b]	1050[b]
330 gal (two-thirds of static maximum resistance)	*18*	**17**	**94**	**306**	**266**	1050[a]
	12	**33**	**108**	**307**	**455**	1050[a]
	11	**51**	**49**	**240**	900[a]	1050[a]
	14	**43**	**61**	**191**	**309**	1050[a]
	17	**57**	**43**	**178**	**416**	**501**
	12	**21**	**98**	**426**	**859**	1050[a]
Average	14	37	76	275	534[b]	959[b]
495 gal (static maximum resistance)	*9*	**27**	**27**	**60**	**215**	**334**
	10	**15**	**64**	**143**	**268**	**468**
	10	**26**	**29**	**100**	**78**	**342**
	12	**17**	**27**	**51**	**81**	**277**
	11	**26**	**39**	**146**	**152**	**1043**
	8	**16**	**35**	**340**	**358**	**524**
Average	10	21	37	140	192	498

Italic values denote nail-head-pull-through with occasional plywood shear, bold values denote bending fatigue failure of nails

[a] No critical failure within 150 s

[b] More than this value

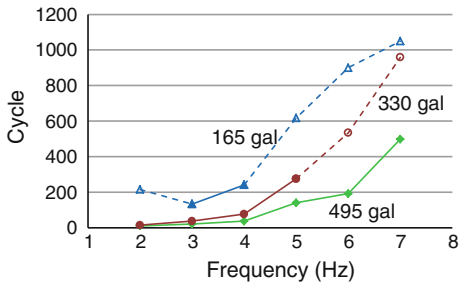

Fig. 10 Cycles at ultimate failures

affects the seismic resistance of entire structures. If the principal frequency components of seismic waves are close to the resonant frequencies after cyclic stiffness degradation of the nailed structural elements, structures are prone to collapse readily under strong earthquakes. If the principal frequency components of seismic waves are close to their resonant frequencies below the damage-limit or serviceability-limit resistance, on the other hand, the structures are initially prone to be damaged, but the resultant stiffness degradation may enable the structures to survive strong earthquakes. This discussion leads to an important conclusion that structural engineers should distinguish between principal frequency components dominant to the ultimate or safety-limit resistance and those dominant to the damage-limit or serviceability-limit resistance [12].

It should be noted that the frequency components resonant to the equivalent frequencies of the nailed joints at their safety-limit may lead them to critical failures when seismic forces act continuously or repeatedly for enough cycles, even if the maximum accelerations do not exceed the accelerations equivalent to the static damage-limit resistance.

In this study, the input frequencies ranged only from 2 to 7 Hz under the restriction due to the capacity of the shaking table. For frequencies higher than 7 Hz, the responsive characteristic can be inferred from the test results shown in Table 1 and Fig. 10. For frequencies lower than 2 Hz, which is probable in actual seismic waves, however, the nailed plywood–timber joints may possibly respond more sensitively and fail more easily. The dynamic tests under steady harmonic waves conducted in this study do not directly yield practical information on the dynamic resistance of nailed plywood–timber joints under

seismic waves. This is because the actual seismic waves consist of various frequencies components and the highest accelerations are not maintained for so many seconds. The next step will be dynamic tests under combined waves consisting of various frequency components [10].

Conclusions

In this study, dynamic tests of nailed plywood–timber joints were carried out under harmonic vibrations from 2 to 7 Hz. The test results showed the following dynamic responsive characteristics of nailed plywood–timber joints:

1. Nailed plywood–timber joints break in low-cyclic bending fatigue failure of nails under dynamic forces in addition to other failure modes. The frequency most severe in this failure mode differs from the frequency most severe in the failure modes typical in static loadings.
2. The dynamic response of nailed plywood–timber joints is clearly dependent upon both input frequency and acceleration.
3. The principal frequency dominant for the safety-limit resistance of the nailed joints should be distinguished from those dominant for the damage-limit resistance.
4. The characteristic responses dependent upon frequency arise from the nonlinear load–slip relationships and the characteristic cyclic stiffness degradation of nailed joints. The cyclic stiffness degradation decreases the resonant frequencies of the same joints, which results in a transition of the dynamic responses.
5. The frequency components resonant to the frequencies corresponding to the safety-limit stiffness may lead the nailed joints to critical failures when dynamic forces act continuously or are repeatedly for enough cycles, even if the input accelerations do not exceed the accelerations equivalent to the static damage-limit resistance.

References

1. Foschi RO, Bonac T (1977) Load–slip characteristics for connections with common nails. Wood Sci 9:118–123
2. Wakashima Y, Hirai T (1993) Hysteretic properties of nailed timber–plywood joints under cyclic loading I. Static cyclic loading test (in Japanese). Mokuzai Gakkaishi 39:1259–1266
3. Wakashima Y, Hirai T (1993) Hysteretic properties of nailed timber–plywood joints under cyclic loading II. Application of the generalized theory of a beam on an elastic foundation (in Japanese). Mokuzai Gakkaishi 39:1377–1385
4. Wakashima Y, Hirai T (1997) Hysteretic properties of nailed timber–plywood joints under cyclic loading III. Revaluation of basic material properties (in Japanese). Mokuzai Gakkaishi 43:417–426
5. Chui YH, Ni C, Jiang L (1998) Finite element model for nailed wood joints under reversed cyclic load. J Struct Eng ASCE 124:96–103
6. Foschi RO (2000) Modeling the hysteretic response of mechanical connectors for wood structures. In: Proceedings of the 6th world conference of timber engineering, Whistler, Canada
7. Meirovitch L (1986) Elements of vibration analysis. MacGraw-Hill, Singapore, p 4
8. Japan Ministry of Land, Infrastructure, Transport and Tourism (2000) Enforce Order No. 81-2, No.82-5 of the Japan Building Standards Act
9. Architectural Institute of Japan (ed) (2006) Standard for structural design of timber structures (in Japanese). Architectural Institute of Japan, Tokyo, pp 50–56, 375
10. Ishiyama Y (2008) Seismic codes and structural dynamics (in Japanese). Sanwa-shoseki Co. Ltd., Tokyo, pp 50–55
11. JSMS Committee on Fatigue of Materials (ed) (2009) Fatigue design for beginners (in Japanese). The Society of Material Science, Kyoto, pp 26–29
12. Hirai T, Sawata K, Awaludin A, Sasaki Y, Uematsu T (2012) Dynamic response of wall-floor joints of wooden light frame constructions under forced harmonic vibrations. J Wood Sci 58:128–134